The Canadian Mineralogist
Vol. 44, pp. 1025-1044 (2006)

CORONAS, SYMPLECTITIC TEXTURES, AND REACTIONS INVOLVING ALUMINOUS MINERALS IN GEDRITE – CORDIERITE – GARNET GNEISS FROM EVERGREEN, FRONT RANGE, COLORADO

ADRIANA HEIMANN[§] AND PAUL G. SPRY

Department of Geological and Atmospheric Sciences, 253 Science I, Iowa State University, Ames, Iowa 50011–3212, U.S.A.

GRAHAM S. TEALE

Teale and Associates, P.O. Box 740, North Adelaide, South Australia 5006, Australia

CARL E. JACOBSON

Department of Geological and Atmospheric Sciences, 253 Science I, Iowa State University, Ames, Iowa 50011–3212, U.S.A.

ABSTRACT

Gedrite – cordierite – garnet gneisses metamorphosed to the upper amphibolite facies near Evergreen, Colorado, are interlayered with sillimanite – biotite – garnet gneisses and contain spectacular corona, symplectite, and pseudomorph textures. Corona textures are characterized by a core of aluminous minerals, including zinc-bearing hercynite (hc), staurolite (st), corundum (crn), cordierite (crd), and relict sillimanite (sil), associated with ilmenite (ilm) and later-formed högbomite (hög). The aluminous minerals ("corona" association) are separated from gedrite (ged), cordierite, garnet (grt), and quartz (qtz) ("matrix" association) by a shell of cordierite such that they are nowhere in contact with gedrite and garnet. Zincian hercynite – cordierite symplectites occur within the inner part of the cordierite shell, whereas staurolite – corundum – cordierite and hercynite – cordierite pseudomorphs mimic the shape of prismatic sillimanite crystals. Textural studies and phase relationships in the system FeO – MgO – Al_2O_3 – SiO_2 ± MnO ± ZnO ± TiO_2 ± S_2 suggest the following reactions, derived from gedrite + sillimanite: ged + sil = crd + grt; ged + sil + sphalerite (sph) = grt + crd + hc + S_2; ged + sil + sph + qtz = grt + crd + hc + crn + S_2; sil + hc = st + crn; grt + sil + crd = st; grt + sil + crd + hc = st; and hc + ilm + crn = hög. These reactions were developed in response to changing physicochemical conditions and enhanced by low diffusivity of aluminum and a low fluid-to-rock ratio. Reactions involving zincian hercynite were developed owing to the presence of sphalerite and preserved by the low diffusivity of aluminum. Högbomite formed later along the retrograde cooling path. Minimum peak conditions of metamorphism were 680°C and 5 kbar on the basis of the stability field of ged + sil + grt. Conditions recorded by the garnet – cordierite geothermometer indicate temperatures of 629–673°C at 5 kbar and 616–659°C at 2 kbar. On the basis of the slope of the garnet- and staurolite-forming reactions, coronas, symplectites, and pseudomorphs formed after peak metamorphism during a clockwise path associated with post-collisional decompression and subsequent cooling of the Yavapai–Mazatzal provinces, probably related with rapid exhumation.

Keywords: gedrite – cordierite – garnet gneiss, zincian hercynite, corona, symplectite, Evergreen, Front Range, Colorado.

SOMMAIRE

Des gneiss à gédrite – cordiérite – grenat équilibrés au faciès amphibolite supérieur près de Evergreen, au Colorado, sont interlités avec des gneiss à sillimanite – biotite – grenat et contiennent des textures en couronnes, des symplectites et des pseudomorphes spectaculaires. Les textures en couronnes possèdent un noyau de minéraux alumineux, avec hercynite zincifère (hc), staurolite (st), corindon (crn), cordiérite (crd), et sillimanite (sil) en reliques, associés à ilménite (ilm) et högbomite (hög) tardive. Les minéraux alumineux (l'association coronitique) sont séparés de la gédrite (ged), cordiérite, grenat (grt), et quartz (qtz) (l'association de la "matrice") par un liseré de cordiérite, de telle sorte qu'ils ne sont nulle part en contact avec gédrite et grenat. Les symplectites à hercynite zincifère + cordiérite se trouvent dans la partie interne du liseré de cordiérite, tandis que les pseudomorphes de staurolite + corundum + cordiérite et hercynite + cordiérite rappèlent la forme des cristaux prismatiques de sillimanite. D'après nos études texturales et les relations de phase dans le système FeO – MgO – Al_2O_3 – SiO_2 ± MnO ± ZnO ± TiO_2 ± S_2, nous préconisons les assemblages suivants, dérivés aux dépens de gédrite + sillimanite: ged + sil = crd + grt; ged + sil + sphalérite (sph) = grt + crd + hc + S_2; ged + sil + sph + qtz = grt + crd + hc + crn + S_2; sil + hc = st + crn; grt + sil + crd

§ *E-mail address*: adrianaheimannr@hotmail.com

= st; grt + sil + crd + hc = st, et hc + ilm + crn = hög. Ces réactions se seraient formées suite aux changements des conditions physicochimiques, et promues par la faible diffusivité de l'aluminium et le faible rapport des volumes de fluide à roche. Les réactions impliquant la hercynite zincifère se sont développées à cause de la présence de la sphalérite et ont été préservées à cause de la faible diffusivité de l'aluminium. La högbomite se serait formée plus tard, par rétrogression lors du refroidissement. Les conditions du paroxysme métamorphique étaient 680°C et 5 kbar, selon le champ de stabilité de ged + sil + grt. Selon le géothermomètre fondé sur grenat + cordiérite, les conditions indiquées auraient été 629–673°C à 5 kbar et 616–659°C à 2 kbar. En fonction de la pente des réactions responsables de la formation du grenat et de la staurolite, les couronnes, textures symplectitiques et pseudomorphes sont apparus après le paroxysme métamorphique lors d'un tracé dans le sens de l'horloge associé à la décompression post-collision et au refroidissement subséquent des provinces Yavapai–Mazatzal, probablement liés à une exhumation rapide.

(Traduit par la Rédaction)

Mots-clés: gneiss à gédrite – cordiérite – grenat, hercynite zincifère, couronne, symplectite, Evergreen, Front Range, Colorado.

Introduction

Gedrite – cordierite or anthophyllite – cordierite rocks are spatially associated with metamorphosed massive sulfide deposits at, for example, Manitouwadge, Ontario (James *et al*. 1978), Orijärvi, Finland (Schneiderman & Tracy 1991), and Palmeiropolis, Brazil (Araujo *et al*. 1995) and may constitute exploration guides to ores of this type. Another potential exploration guide to metamorphosed Proterozoic massive sulfides includes their spatial association with nodular sillimanite rocks and unusual rutile- and topaz-bearing sillimanite rocks (*e.g.,* Willner *et al*. 1990). Petersen *et al*. (1989) proposed that gedrite – cordierite rocks, nodular sillimanite rocks, and rutile- and topaz-bearing gneisses may be products of premetamorphic hydrothermal alteration. The current investigation is part of a larger study that concerns the spatial and genetic relationships of zincian-spinel-bearing rocks to metamorphosed massive sulfides in Colorado (Heimann *et al*. 2005). In detail, the present study focuses on outcrops of gedrite – cordierite – garnet gneiss in the Evergreen area of central Colorado (Gable & Sims 1969), which are spatially associated with nodular sillimanite rock and rutile- and topaz-bearing gneiss (Marsh & Sheridan 1976).

Gedrite – cordierite – garnet gneiss of the Evergreen area contains corona, symplectite, and pseudomorph textures that involve aluminous and zinc-bearing minerals. Similar textures elsewhere have proven to be important in deciphering pressure–temperature trajectories in rocks metamorphosed to the amphibolite or granulite facies (Robinson & Jaffe 1969, Stoddard 1979, Hudson & Harte 1985, Baker *et al*. 1987, Schumacher & Robinson 1987, Earley & Stout 1991, Spear 1993, Ouzegane *et al*. 1996). The main aim of the current study is to evaluate the origin of coronas, symplectites, and pseudomorphs involving aluminous minerals in gedrite – cordierite – garnet gneiss. Detailed petrographic observations, mineral compositions, and phase relationships in the system $FeO – MgO – Al_2O_3 – SiO_2 \pm MnO \pm ZnO \pm TiO_2 \pm S_2$ are utilized to determine the metamorphic reactions that took place in these rocks. Metamorphic conditions are evaluated on the basis of silicate stabilities, various exchange-geothermometers (garnet – cordierite, spinel – cordierite, and spinel – sillimanite – cordierite – quartz), and the orthoamphibole solvus.

Regional And Local Geological Setting

The Evergreen area is located in the east-central part of the Front Range, approximately 30 km west of Denver, Colorado (Fig. 1). At the regional scale,

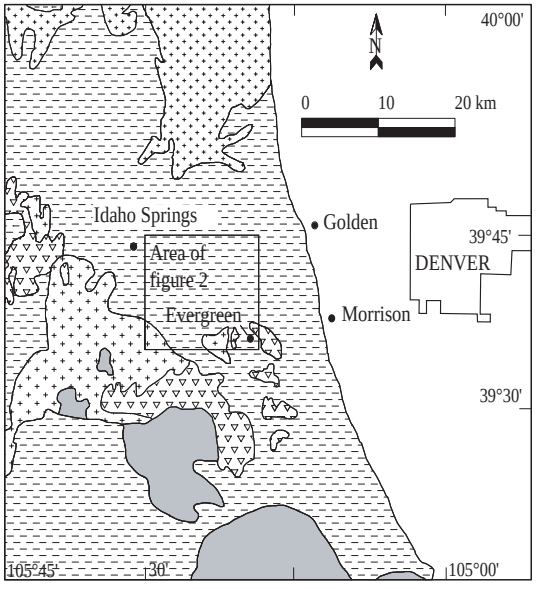

FIG. 1. Geological map of the Evergreen area, east-central Front Range (after Marsh & Sheridan 1976). Map patterns: Colorless: Cenozoic, Mesozoic and Paleozoic sedimentary rocks, grey: Pikes Peak Granite (1,040 m.y.), triangles: Silver Plume Granite (1,440 m.y.), crosses: Boulder Creek Granite and related rocks (1,710 m.y.), dashed lines: metamorphic rocks, solid line: lithological contact.

it lies within the 1.8–1.7 Ga Yavapai Province, which is composed of juvenile volcanic-arc crust near its southern contact with the crustal 1.7–1.6 Ga Mazatzal Province (Condie 1982, Benett & DePaolo 1987, Karlstrom 1998, Karlstrom & Humphreys 1998). The exact location of the boundary zone between these terranes is the subject of debate, but Shaw & Karlstrom (1999) proposed that at about 1.70 Ga, collision between the two portions of crust produced shear zones in association with the emplacement of the older Yavapai rocks over the Mazatzal Province along a low-angle thrust system.

Gedrite – cordierite – garnet gneiss in the study area occurs as two lensoid bodies, up to 40 m wide, which extend intermittently for over 300 m in a sequence of sillimanite – biotite gneisses containing coarse garnet- and cordierite-bearing layers. Also present in the study area are feldspathic, hornblende, rutile-bearing, and calc-silicate gneisses and amphibolites (Figs. 1, 2). Sillimanite-rich gneiss, composed mainly of sillimanite, biotite, and muscovite, commonly contains white rounded pods of feldspar and quartz, up to 4 cm in length. These rocks resemble the nodular sillimanite or andalusite rocks found throughout Colorado in and around Proterozoic metamorphosed massive sulfide deposits (Heimann *et al*. 2005). Gedrite – cordierite – garnet gneiss constitutes just one of many occurrences of cordierite-bearing gneiss in the Front Range that have been metamorphosed to the upper amphibolite facies and subjected to at least two Proterozoic episodes of folding (Gable & Sims 1969, Marsh & Sheridan 1976). The first period of deformation produced broad open folds and was responsible for the west-to-northwest trend of the rocks, whereas the second episode of folding generated structures oriented north–northwest to north–northeast. High-grade metamorphism contemporaneous with these two episodes of folding was dated at 1,700 to 1,775 Ma by Hedge *et al*. (1967) using Rb–Sr and U–Pb techniques. The Boulder Creek Granite pluton, which occurs to the west and south of the gedrite – cordierite – garnet rocks, was emplaced at 1,709 ± 40 Ma (Hedge 1969, Premo & Fanning 2000) and was followed by intrusion of the Silver Plume Granite at approximately 1,450 Ma (Hedge *et al*. 1967, 1986, Hedge 1969, Marsh & Sheridan 1976). The last Proterozoic plutonic event occurred when the anorogenic Pikes Peak Granite batholith was emplaced at 1,040 ± 10 Ma (Hedge 1969). Brittle deformation, which controlled the location of the Colorado Mineral Belt (Tweto & Sims 1963), produced northeast-oriented shear zones. This period of deformation was followed by northwest- and north–northeast-trending faulting and the so-called "breccia reefs" of Lovering & Goddard (1950), which were precursor structures to the Laramide orogeny (75–45 Ma).

TABLE 1. MINERAL ASSEMBLAGES IN GEDRITE–CORDIERITE–GARNET AND GARNET – SILLIMANITE – BIOTITE GNEISSES FROM EVERGREEN

Sample	99CO 64	99CO 64B	99CO 65A	99CO 65B	AHCO 5	AHCO 6	AHCO 7	99CO 63	AHCO 3
Matrix assemblage									
Gedrite	×	×	×	×	×	×	×	×	
Cordierite	×	×	×	×	×	×	×	×	
Garnet		×	×	×	×	×	×	×	×
Quartz	×	×	×		×	×		×	×
Ilmenite	×	×	×	×	×	×	×	×	×
Hematite				×			×		×
Biotite [1]	×			×	×	×	×	×	×
Chlorite [1]	×	×	×	×	×	×	×	×	
White mica [2]	×		×	×		×	×	×	
Sillimanite									×
Sulfides [2]								×	
Plagioclase [3]	×								
Corona assemblage									
Hercynite	×	×	×	×	×	×	×		
Staurolite	×	×	×						
Sillimanite	×	×							
Cordierite	×	×	×	×	×	×	×		
Corundum	×	×	×	×		×			
Quartz	×	×	×	×	×	×	×		
Högbomite	×	×	×	×		×	×		
Ilmenite	×	×	×	×	×	×	×		
Magnetite						×	×		
Chlorite[1]		×							
Accessory minerals									
Apatite			×		×			×	×
Zircon					×			×	×

[1] Retrograde minerals, [2] Sphalerite, pyrite, and chalcopyrite, [3] Inclusion of plagioclase ($An_{\leq 51}$) in cordierite.

Petrography, Mineral Assemblages and Reaction Textures

Gedrite – cordierite – garnet gneiss is characterized by a grano-lepidoblastic texture composed of coarse (up to 3 cm in length), dark green elongate crystals of gedrite, dark violet grains of cordierite (up to 2 cm in length), and red porphyroblasts of garnet (up to 3 cm in diameter).

A closer observation indicates that the gedrite – cordierite – garnet gneiss contains coronas, symplectitic intergrowths, pseudomorphs, and reaction rims (Fig. 3). These coronas separate the mineral assemblages in the gneiss into two textural associations, a "corona" association and a "matrix" association (Table 1). The corona association, composed of different combinations of cordierite, hercynite, corundum, staurolite, relict sillimanite, högbomite, ilmenite, and minor quartz, is separated from the matrix association composed of gedrite, cordierite, garnet, and accessory ilmenite and quartz, by a corona of cordierite (Table 1). The following mineral associations occur from the center of the corona or "enclave" (terminology of Robinson & Jaffe 1969) toward the matrix: sillimanite – aluminous minerals (staurolite – corundum – hercynite) – cordierite shell

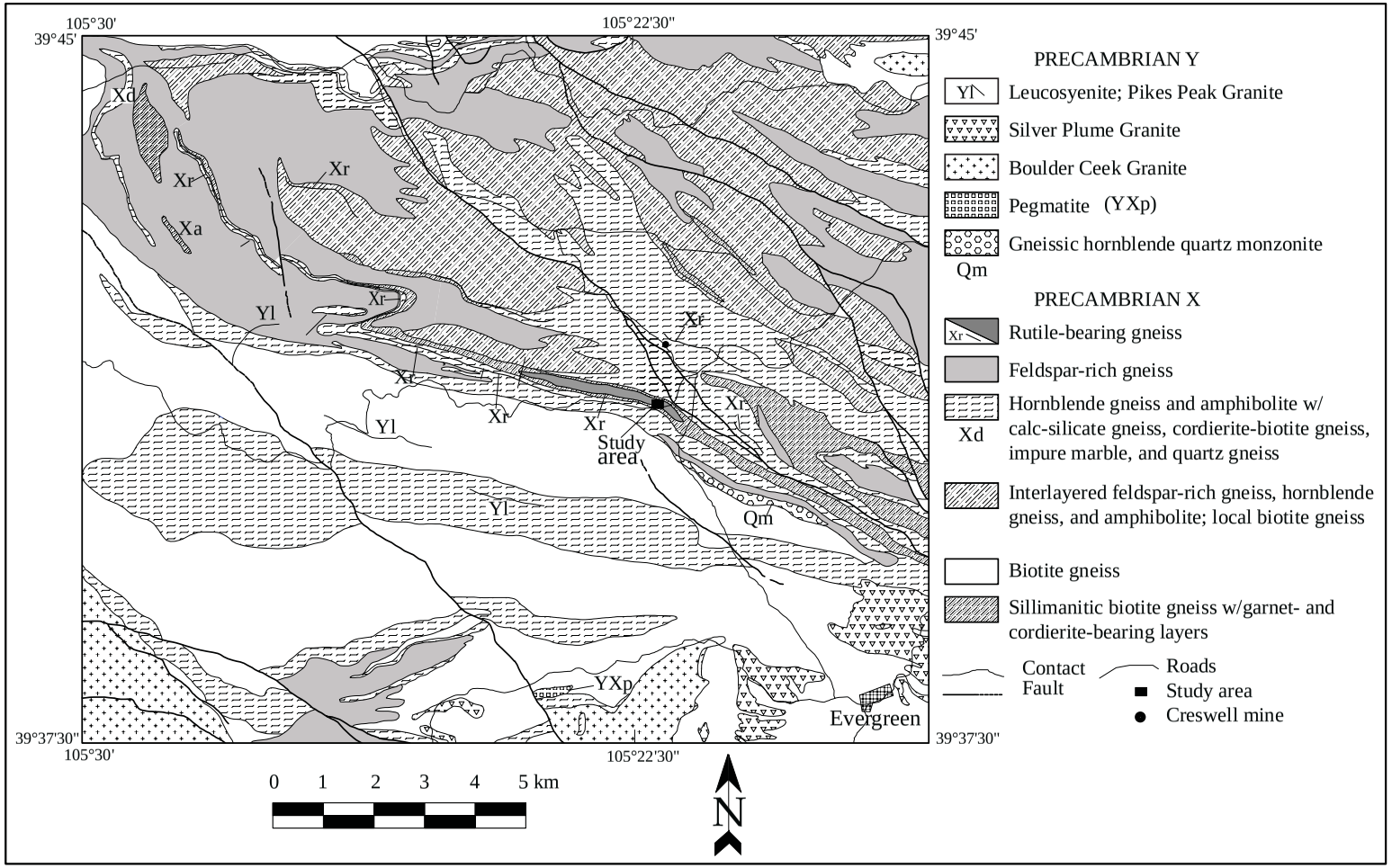

FIG. 2. Detailed geological map of the Evergreen area, east-central Front Range, showing the location of the study area (after Marsh & Sheridan 1976). Terminology for the Precambrian units is that of Taylor *et al.* (1975a, b).

– gedrite – (garnet – cordierite – gedrite). Within the enclaves, the minerals lack any deformational feature, in contrast to the weakly oriented gedrite and the fractured nature of garnet in the matrix. Minor amounts of retrograde pale brown biotite (up to 0.2 mm in length) cross-cut gedrite and garnet and formed after these minerals. Pale green chlorite partially replaced biotite, gedrite, and garnet, and along with white mica, forms part of the breakdown of cordierite.

Gedrite – cordierite – garnet – quartz matrix association

Gedrite forms coarse acicular to prismatic crystals that show an undulose extinction and subgrain development. Gedrite also appears as fine-grained euhedral, short prismatic, and elongate tabular crystals included in cordierite (Figs. 4a, b). Large porphyroblasts of garnet form highly poikilitic sieve-textured and fractured crystals that contain aligned quartz and cordierite inclusions (Fig. 4a). A minor amount of smaller crystals of garnet, up to 0.2 mm in diameter, occurs as inclusions in cordierite, and garnet porphyroblasts are, in places, surrounded by a corona of cordierite.

Cordierite occurs as individual crystals with triple junctions at 120° in contact with gedrite and garnet, but it also nucleated on pre-existing gedrite as optically continuous, xenomorphic crystals, as well as thin elongate grains that fill fractures and cleavage planes in gedrite (Fig. 4b) and garnet. Gedrite, garnet, ilmenite, quartz, and minor apatite and zircon, as well as rare plagioclase (only one grain identified herein) inclusions occur in matrix cordierite.

Quartz occurs as inclusions within cordierite and garnet as well as individual crystals in contact with gedrite, garnet, and cordierite. Ilmenite, which is the dominant oxide in these rocks, is present as anhedral to euhedral crystals (up to 0.8 mm in length) in contact with and as inclusions in garnet, cordierite, and gedrite (Fig. 4a). Traces of secondary hematite are intergrown with ilmenite. Trace amounts of ilmenite, sphalerite, pyrite, and chalcopyrite occur in one sample (99CO–63) devoid of enclaves.

Cordierite – hercynite – corundum – staurolite – sillimanite – högbomite corona association

The corona association consists of a central nucleus of Al-rich minerals surrounded by a halo of cordierite (Fig. 4c). In this association, cordierite forms equilibrium mosaics composed of smaller crystals than in the matrix. These crystals exhibit triple junctions at approximately 120°. Relict, corroded sillimanite is locally preserved in the center of the nucleus, in contact with hercynite, corundum, cordierite, and ilmenite (Fig. 4d). In places, these minerals mimic the elongate sections of sillimanite, which they have replaced (Figs. 4d, e, f). Hercynite, the most abundant aluminous mineral, occurs as isolated dark green and rare pale green anhedral to subhedral crystals (0.1 mm in length), and as symplectitic intergrowths with cordierite. In some samples, hercynite contains abundant tiny opaque inclusions of magnetite or ilmenite, either concentrated in the rim or distributed within the host crystal. Hercynite – cordierite symplectites occur locally between the central crystals of sillimanite and the cordierite shell (Figs. 4d, e). Within the intergrowth, cordierite predominates over hercynite. The small worm-like symplectites are oriented approximately perpendicular to the corona–matrix interface and parallel to the long side of the sillimanite crystal.

Corundum, which varies from small colorless subhedral crystals to less common larger pale blue xenomorphic poikilitic crystals (up to 1 mm in size) enclosing cordierite, characteristically exhibits a corroded rim and contains inclusions of ilmenite (Figs. 4e, f). A few inclusions of hercynite were also identified in corundum. Corundum is also commonly associated with ilmenite and hercynite in rare and complex intergrowths in which both minerals contain small inclusions of each other.

Staurolite forms yellow euhedral short prismatic crystals (Fig. 4g) and xenomorphic, colorless to pale yellow crystals (Fig. 4f). In the latter case, corundum – staurolite – cordierite and hercynite – cordierite formed rectangular "mosaic"-like pseudomorphs, which partially replaced sillimanite (Fig. 4f). In these domains, sillimanite is in direct contact with hercynite, whereas corundum contains inclusions of sillimanite and occurs in contact with it in only one location. Where individual crystals of staurolite and hercynite are present, they are not in mutual contact, but are separated by ilmenite or cordierite. The only place where hercynite occurs in contact with staurolite is where it is found as tiny inclusions in the staurolite.

Ilmenite occurs in the coronas as xenomorphic to subidiomorphic crystals associated with the aluminous minerals. It is included in cordierite, staurolite and hercynite, and contains euhedral inclusions of corundum. In some samples, an intergrowth or a replacement among ilmenite, hercynite, corundum, and högbomite is present. Hercynite occurs in close proximity to corundum, but is separated from it by ilmenite or högbomite (or both). In places, dark brown högbomite (up to 0.05 mm in size) appears as a thin rim along the contact between hercynite and ilmenite where spatially associated with corundum (Fig. 4h).

Mineral Compositions

Analytical procedure

Compositions of silicates and oxides were determined using an ARL–SEMQ electron microprobe in the Department of Geological and Atmospheric Sciences at Iowa State University. Accelerating voltage was set at 15 kV, and specimen current at 20 nA. Natural and

FIG. 3. Scanned image of a thin section showing a corona structure in gedrite – cordierite – garnet gneiss composed of a core of aluminous minerals (hercynite, staurolite, corundum, sillimanite, cordierite, and högbomite) plus ilmenite separated from gedrite and almandine by a moat of cordierite.

synthetic silicates and oxides were used as standards. Representative results of the analyses are given in Tables 2 and 3, and all compositions are presented in Appendix 3 of Heimann (2002).

Amphibole

Thirty-nine analyses of amphiboles were obtained, with representative results given in Table 2. Formulas were determined on the basis of 23 oxygen atoms, and the proportion of Fe^{3+} was calculated following the procedure of Robinson *et al.* (1982). Using the International Mineralogical Association classification of Leake *et al.* (1997), amphiboles from Evergreen fall in the gedrite and ferrogedrite fields in a plot of Si *versus* $Mg/(Mg + Fe^{2+})$ (Fig. 5a). Values of X_{Mg} [$Mg/(Mg + Fe^{2+})$] range from 0.46 to 0.57, with two outlier values of 0.68 and 0.71. The amphiboles contain more alkalis and less ^{IV}Al [$(Na + K) < 0.5$, $^{IV}Al = 1.02$ to 1.89 *apfu*)] than $\square Mg_5Al_2Si_6Al_2O_{22}(OH)_2$, the ideal formula for gedrite (Fig. 5b). The edenite to tschermakite ratio (calculated as $^{A}(Na + K)/[^{IV}Al - {}^{A}(Na + K)]$, after Damman 1989) ranges from 0.22 to 0.46. The proportion of ^{VI}Al ranges from 0.70 to 1.29 (with two values of 0.32 and 0.40; Fig. 5c), and the variation in the occupancy of the *A* site is 0.25 to 0.53 (Fig. 5b).

Cordierite

Representative results of the electron-microprobe analyses of cordierite from corona and matrix assemblages show them to be essentially the same (Table 2). Cordierite is the most magnesian mineral present in gedrite – cordierite – garnet rocks [$Mg/(Mg + Fe^{Tot})$ in the range 0.7 to 0.8]. The content of Mg ranges from 8.5 to 13.5 wt.% MgO, whereas the Fe content varies between 5.6 and 8.16 wt.% FeO. The Al_2O_3 content ranges from 31.90 to 37.60 wt.%, whereas ^{VI}Al and ^{IV}Al vary between 2.7 and 3.19 and from 0.9 to 1.38 *apfu*, respectively.

TABLE 2. REPRESENTATIVE CHEMICAL COMPOSITIONS OF GEDRITE, GARNET, AND CORDIERITE FROM EVERGREEN

Mineral	Gedrite			Garnet			Cordierite	
	99CO 65B	99CO 64		99CO 64B	99CO 65B		99CO 64B[2]	99CO 65B[3]
SiO_2 wt.%	45.56	45.57	SiO_2	36.50	37.92	SiO_2	48.23	48.41
TiO_2	0.23	0.12	TiO_2	0.01	0.01	TiO_2	0.01	0.00
Al_2O_3	12.99	12.46	Al_2O_3	22.13	21.09	Al_2O_3	34.36	34.55
Cr_2O_3	0.00	0.02	Cr_2O_3	0.00	0.00	Cr_2O_3	0.00	0.03
FeO	23.98	24.33	FeO	33.25	32.63	FeO	6.10	6.22
MnO	0.40	0.39	MnO	1.56	1.91	MnO	0.12	0.09
ZnO	0.03	0.05	MgO	3.91	6.63	ZnO	0.03	0.00
MgO	13.31	13.35	CaO	1.78	1.72	MgO	9.94	9.19
CaO	0.46	0.46	Na_2O	0.03	0.00	CaO	0.00	0.03
Na_2O	1.41	1.20				Na_2O	0.09	0.20
K_2O	0.01	0.01	Total	99.17	101.91	K_2O	0.00	0.02
F	0.38	0.37	FeO[1]	32.78	29.48	F	0.00	0.14
Cl	0.00	0.02	Fe_2O_3[1]	0.53	3.50	Cl	0.00	0.01
Total	98.76	98.35	Total[1]	99.22	102.26	Total	98.88	98.89
Si *apfu*	6.716	6.721	Si	2.935	2.934	Si	4.879	4.861
Ti	0.026	0.009	Ti	0.001	0.001	Ti	0.001	0.000
^{IV}Al	1.284	1.279	^{IV}Al	0.065	0.066	^{IV}Al	1.121	1.139
^{VI}Al	0.971	0.869	^{VI}Al	2.031	1.856	^{VI}Al	2.973	2.947
Cr	0.000	0.006	Cr	0.000	0.000	Fe	0.516	0.522
Fe^{3+}	0.000	0.054	Fe^{3+}	0.032	0.204	Mn	0.010	0.008
Fe^{2+}	2.956	2.981	Fe^{2+}	2.204	1.908	Zn	0.002	0.000
Mn	0.050	0.055	Mn	0.106	0.125	Mg	1.499	1.376
ZnO	0.001	0.001	Mg	0.469	0.765	Ca	0.000	0.003
Mg	2.925	2.955	Ca	0.153	0.143	Na	0.018	0.039
Ca	0.073	0.071	Na	0.005	0.000	K	0.000	0.003
^{A}Na	0.403	0.332						
^{A}K	0.002	0.000	Alm	75.16	56.30	Σ cat	11.019	10.898
			Adr	1.62	6.04			
^{A}Sum	0.405	0.332	Grs	3.61	0.00	X_{Mg}	0.74	0.72
			Prp	15.98	32.37			
Cl	0.000	0.008	Sps	3.62	5.30			
F	0.177	0.303						
			$X_{Fe^{3+}}$	0.05	0.05			
Σ cat	16.000	15.975	X_{Mg}	0.50	0.50			
			X_{Fe}	0.75	0.65			
X_{Mg}	0.16	0.26						
			Fe^{2+}/Mg	4.70	2.49			

[1] Calculated; [2] Matrix cordierite; [3] Corona cordierite. The calculated proportions of cations are based on 23, 12, and 18 atoms of oxygen for gedrite, garnet and cordierite, respectively.

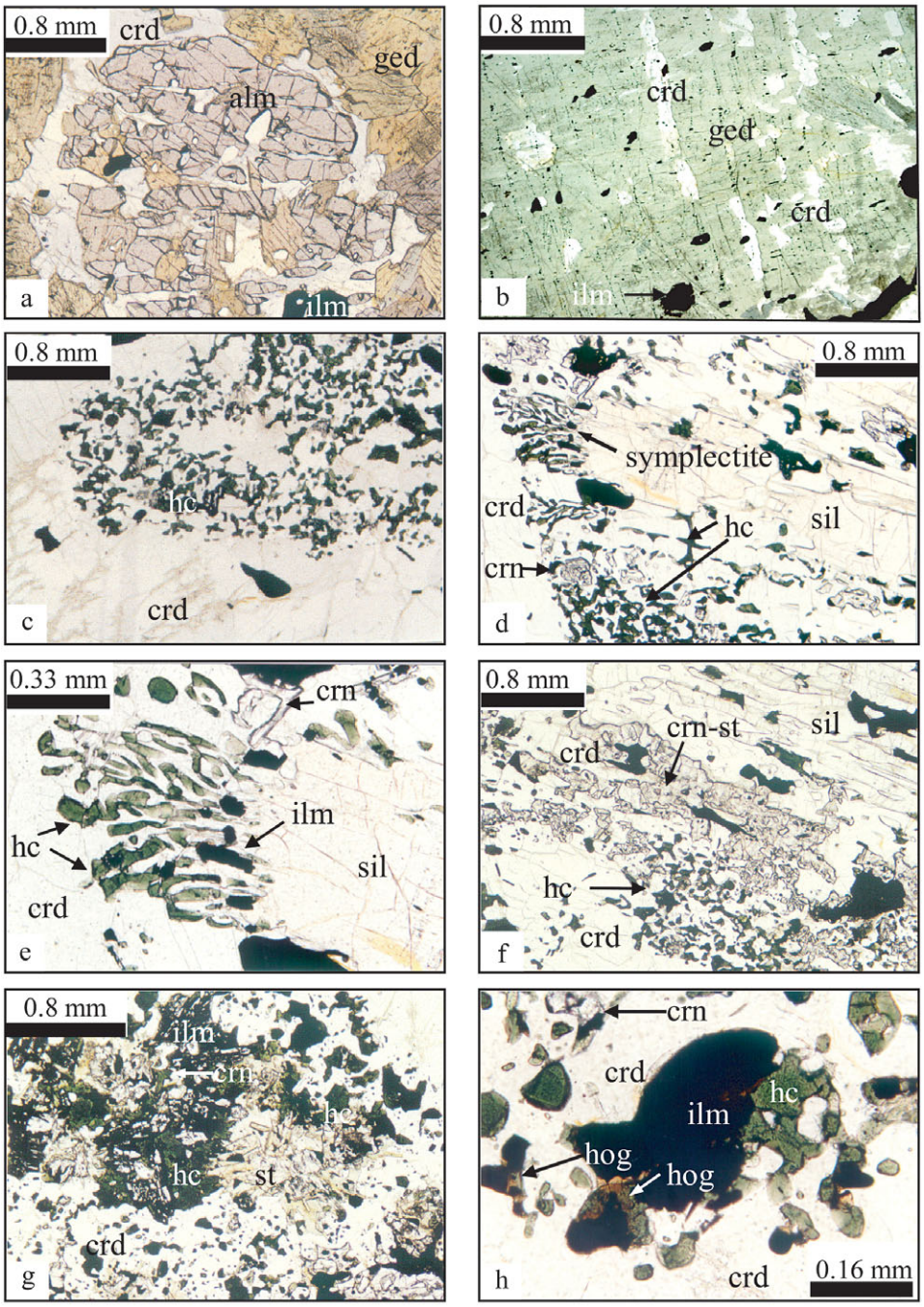

FIG. 4. Photomicrographs in plane-polarized transmitted light of: a. Almandine garnet (alm) surrounded by cordierite (crd), gedrite (ged), and ilmenite (ilm). b. Gedrite cross-cut by cordierite through fractures. c. Corona structure showing the core composed of hercynite (hc) and cordierite surrounded by a corona of cordierite. d. Hercynite – cordierite symplectites in contact with relict sillimanite (sil) and corundum (crn) – cordierite – hercynite in contact with cordierite at the edge of a corona. e. Hercynite – cordierite symplectites in contact with corundum, ilmenite, and relict sillimanite, and a cordierite collar. f. Hercynite – cordierite and corundum – staurolite (st) – cordierite pseudomorphs after sillimanite. g. The core of a corona composed of hercynite, euhedral staurolite, cordierite, corundum, and ilmenite. h. Reaction rim of högbomite (hog) along the contact between ilmenite and hercynite.

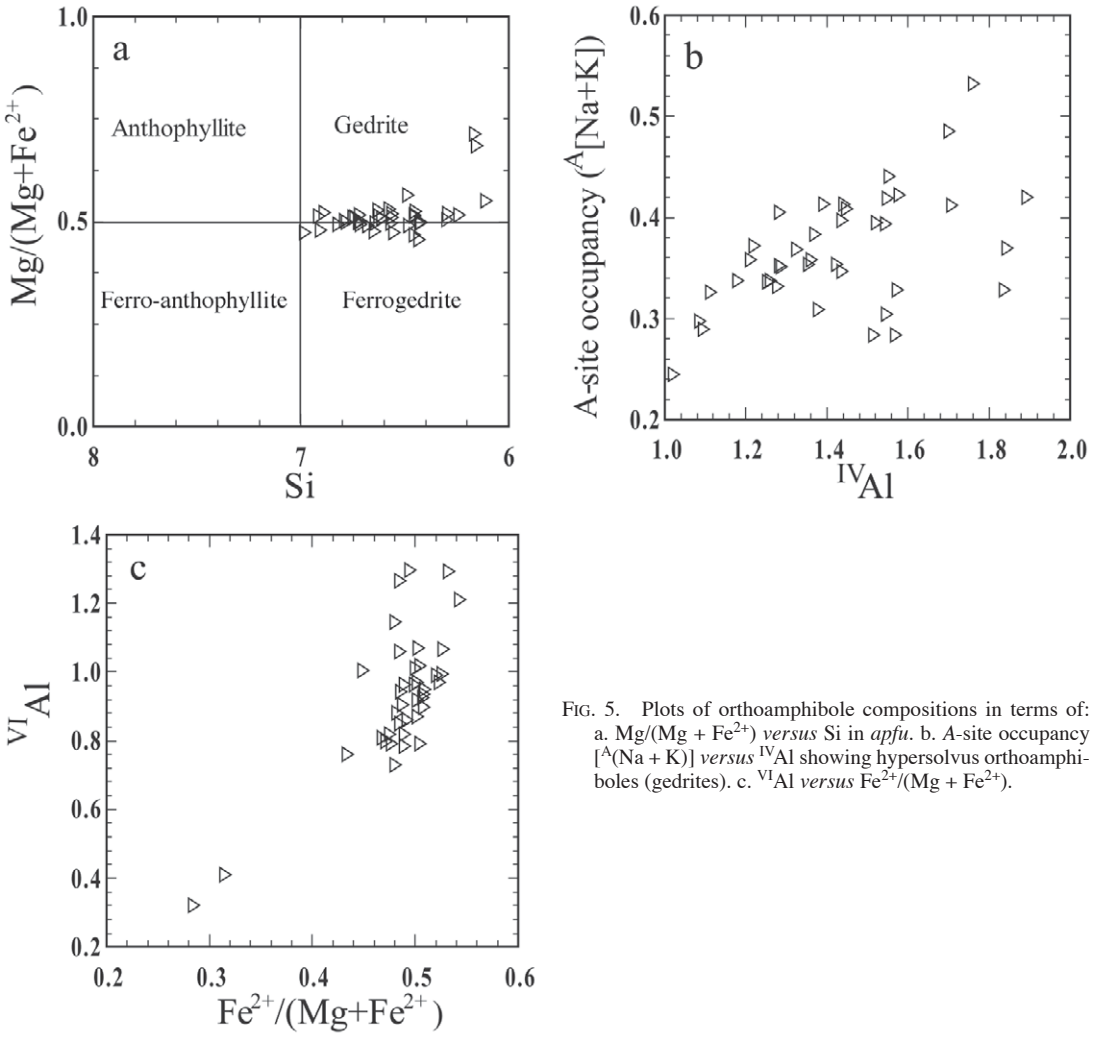

FIG. 5. Plots of orthoamphibole compositions in terms of: a. Mg/(Mg + Fe^{2+}) *versus* Si in *apfu*. b. *A*-site occupancy [^{A}(Na + K)] *versus* ^{IV}Al showing hypersolvus orthoamphiboles (gedrites). c. ^{VI}Al *versus* Fe^{2+}/(Mg + Fe^{2+}).

Garnet

Twenty-six analyses of cores and rims of garnet grains show that they are individually homogeneous (Table 2). End members were calculated following Rickwood (1968), whereas the proportion of ferric to ferrous iron was determined using the technique of Droop (1987). Almandine (Alm), pyrope (Prp), spessartine (Sps), grossular (Grs), and andradite (Adr) contents vary from $Alm_{56.3}$ to $Alm_{79.7}$, $Prp_{15.3}$ to $Prp_{32.4}$, $Sps_{1.9}$ to $Sps_{5.3}$, $Grs_{0.0}$ to $Grs_{5.9}$, and Adr_{0} to $Adr_{6.3}$, respectively. The amount of ferric iron present in garnet is low (0–0.26 *apfu*). Values of X_{Mg} range from 0.15 to 0.26, indicating that garnet is the most iron-rich silicate mineral in the Evergreen rocks.

Staurolite

Iron and magnesium contents of staurolite are 12.5–13.4 wt.% FeO and 1.7–2.2 wt.% MgO, respectively (Table 3); values of X_{Mg} range from 0.19 to 0.25, with the lowest X_{Mg} value being higher than the lowest value for garnet. Staurolite also contains minor amounts of zinc (0.49–0.89 wt.% ZnO), which may have helped stabilize staurolite to the upper amphibolite facies (Ribbe 1982). These Zn contents are similar to or less than those of staurolite associated with cordierite – orthoamphibole rocks in or adjacent to massive sulfide deposits elsewhere (Geco, Ontario: Spry 1982; Palmeiropolis, Brazil: Araujo *et al.* 1995). However, compared to staurolite from gedrite – cordierite localities unrelated to massive sulfides (*e.g.,* New Hampshire, Schumacher

& Robinson 1987), staurolite from Evergreen contains slightly higher amounts of Zn.

Zincian hercynite

Spinel from Evergreen consists mainly of zincian hercynite and rare ferroan gahnite ($ghn_{6.5–44}hc_{41–74}spl_{13–32}$) that contains 3.57 to 19.48 wt.% ZnO and possesses X_{Mg} values ranging from 0.18 to 0.29 (Table 3, Fig. 6). Compared to zincian spinel spatially associated with massive sulfide deposits, the spinel from Evergreen contains less zinc and falls in the field of "aluminous metasediments" of Spry & Scott (1986) and in the field of "unaltered and hydrothermally altered Fe–Al-rich metasediments and metavolcanics" of Heimann *et al*. (2005). No compositional zoning was detected within individual crystals.

Högbomite

The Zn content of högbomite, ($[Fe,Mg,Zn]_5Al_{16}TiO_{30}[OH]_2$), ranges from 1.67 to 8.62 wt.% ZnO, with an average of about 3 wt.% ZnO (Table 3). Values of X_{Mg} vary from 0.17 to 0.29, whereas Fe and Mg contents range between 20.2 and 26.9 wt.% FeO, and between 2.2 and 5.2 wt.% MgO, respectively, thus showing that högbomite from Evergreen is among the most iron-rich yet reported (Table 3). The Zn:Fe ratio of hercynite is greater than that for högbomite; parallel tie-lines between coexisting högbomite and hercynite pairs suggest that equilibrium existed between these minerals (Fig. 6).

TABLE 3. REPRESENTATIVE CHEMICAL COMPOSITIONS OF SPINEL, HÖGBOMITE, AND STAUROLITE FROM EVERGREEN

Mineral	Spinel		Högbomite		Staurolite	
	99CO64	99CO64B	99CO64	99CO655	99CO64	99CO64
SiO_2 wt.%	0.04	0.06	0.01	0.94	27.05	26.82
TiO_2	0.00	0.03	4.93	5.76	0.23	0.19
Al_2O_3	58.06	58.06	60.17	57.07	55.62	55.64
Cr_2O_3	0.06	0.01	0.00	0.31	0.00	0.00
FeO	20.92	31.85	23.79	26.37	11.98	12.97
MnO	0.14	0.17	0.11	0.09	0.13	0.25
ZnO	18.09	4.61	7.45	2.76	0.82	0.54
MgO	3.49	5.32	2.96	4.61	2.02	1.85
CaO	0.02	0.05	0.01	0.00	0.00	0.00
Na_2O	0.00	0.18	0.00	0.09	0.09	0.00
K_2O	0.00	0.01	0.02	0.01	0.10	0.01
F	0.00	0.00	0.00	0.00	0.00	0.00
Cl	0.02	0.02	0.00	0.01	0.01	0.01
Total	100.83	100.36	99.46	98.00	98.05	98.27
Si *apfu*	0.001	0.002	0.001	0.203	7.791	7.732
Ti	0.000	0.001	0.800	0.940	0.051	0.041
Al	1.970	1.939	15.294	14.589	18.877	18.904
Cr	0.001	0.000	0.000	0.053	0.000	0.001
Fe	0.504	0.755	4.291	4.784	2.884	3.126
Mn	0.003	0.004	0.021	0.017	0.031	0.060
Zn	0.384	0.096	1.187	0.442	0.174	0.115
Mg	0.150	0.225	0.953	1.489	0.869	0.793
Ca	0.000	0.001	0.001	0.000	0.000	0.000
Na	0.000	0.010	0.000	0.037	0.050	0.000
K	0.000	0.000	0.006	0.001	0.035	0.002
F	0.000	0.000	0.000	0.000	0.000	0.000
Cl	0.001	0.001	0.000	0.003	0.004	0.004
Total	3.014	3.034	22.554	22.56	30.766	30.778
X_{Mg}	0.23	0.23	0.18	0.24	0.23	0.20

The proportion of atoms, expressed in atoms per formula unit (*apfu*), is calculated on the basis of four (spinel), 31 (högbomite) and 48 (staurolite) atoms of oxygen.

Corundum, sillimanite, ilmenite, and plagioclase

Analyses of corundum show that it consists of essentially pure Al_2O_3, with up to 0.99 wt.% FeO, whereas relict crystals of sillimanite located in the core of the corona structures contain up to 2.2 wt.% Fe_2O_3 and up to 0.5 wt.% MgO. Ilmenite contains up to 0.13 wt.% ZnO, 0.80 wt.% MnO, and 0.16 wt.% MgO. A single tiny crystal of plagioclase, with a composition An_{65} to An_{81}, was found as an inclusion in matrix cordierite.

Phyllosilicates

Biotite, which grew at the expense of gedrite during retrograde metamorphism, exhibits uniform compositions (Deer *et al*. 1966), with values of X_{Mg} in the range 0.66–0.71. Values of ^{IV}Al and ^{VI}Al, calculated on the basis of 22 atoms of oxygen, range from 2.43 to 2.62 and from 0.26 to 0.68, respectively. Chlorite, like biotite, is a product of retrograde metamorphism. It possesses a high Mg content and almost the same X_{Mg} as biotite ($0.66 < X_{Mg} < 0.70$).

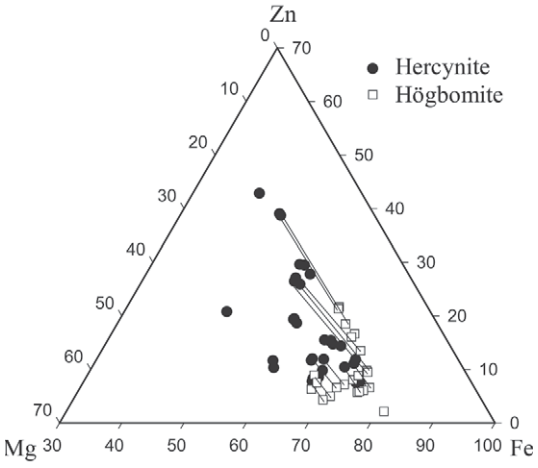

FIG. 6. Plot showing compositions of hercynite and coexisting högbomite in terms of Zn, Mg, and Fe. Tie-lines join coexisting minerals.

Phase Relationships

The mineral compositions recorded for the gedrite – cordierite – garnet rocks from Evergreen can be described within the system $SiO_2 – TiO_2 – Al_2O_3 – FeO – MnO – MgO – ZnO – CaO – Na_2O – K_2O – H_2O$. However, this system can be simplified following the procedure of Schumacher & Robinson (1987) and Robinson & Jaffe (1969) by first removing H_2O, which is considered to be an excess and mobile component. To make the system suitable for representing mineral assemblages on triangular diagrams and balancing metamorphic equilibria, it can be further simplified by ignoring the minor components CaO, MnO, and Na_2O, as only small amounts of CaO and MnO are present in garnet, and the same is true for Na_2O and MnO in gedrite. The component MnO is taken into account in reactions that involve garnet. Considerable amounts of TiO_2 are present only in ilmenite and later-formed högbomite; TiO_2 is, therefore, treated as an accessory inert component except in reactions involving these two minerals. ZnO is considered here as an active component in reactions involving hercynite, staurolite, and högbomite, but as an inert constituent in all remaining reactions. As biotite is present in only minor amounts as a late phase and represents the only potassic mineral present, the K_2O component is not considered further. Chemographic relationships are therefore reduced to the system $FeO – MgO – Al_2O_3 – SiO_2$ (FMAS). For the purpose of graphically representing subassemblages in two dimensions, the chemical composition of analyzed minerals can be plotted projecting from excess components like SiO_2, Al_2O_3, or Al_2SiO_5, which are represented by quartz, corundum, and sillimanite, respectively (Thompson 1957, Greenwood 1975, Robinson & Jaffe 1969).

Using the procedure of Robinson & Jaffe (1969), chemographic relationships are schematically shown in $SiO_2 – (FeO + MgO) – Al_2O_3$ subspace, in which cordierite, gedrite, garnet, hercynite, sillimanite, staurolite, and corundum are plotted with tie-lines joining coexisting phases (Fig. 7a). The presence of the components ZnO, CaO, NaO, and MnO, which are not represented here, adds extra variables to the number of phases that can be stable under the same set of conditions and requires a series of triangular plots to show the observed subassemblages. Most importantly, ZnO, which is present in hercynite and staurolite, is not considered in Figure 7a. A three-dimensional representation with ZnO as a component (five components if FeO and MgO are considered separately) would allow the coexistence of the subassemblages hercynite – sillimanite – cordierite, corundum – cordierite, and staurolite – cordierite [or the five-phase assemblage sillimanite – hercynite – cordierite – corundum – staurolite (Figs. 4e, f)] without producing crossing tie-lines, as observed in Figure 7a. This subcomposition space is illustrated by the tetrahedron $SiO_2 – (FeO + MgO) – Al_2O_3 – ZnO$ [S – (F + M) – A – Z] in Figure 7b, a schematic representation in which staurolite and hercynite are shown. In this diagram, the addition of the ZnO component, located behind the plane containing S – (F + M) – A, in conjunction with the combination of FeO and MgO, allows for the representation of an assemblage such as corundum – hercynite – cordierite – sillimanite. Thus, for a given bulk-rock composition, ZnO increases the number of stable minerals and the stability fields of Zn-bearing mineral phases.

An alternative approach for showing chemographic relationships in more complex systems is to project from an extra phase following the method of Thompson (1957) and Greenwood (1975). One possibility consists of projecting from sillimanite onto the planes $SiO_2 – MgO – FeO$ or $SiO_2 – MgO – (FeO + ZnO + MnO)$. Such a projection was used by Robinson & Jaffe (1969) and Schumacher & Robinson (1987) to represent gedrite, cordierite, staurolite, corundum, and spinel compositions and to show the sequence of reactions that produced aluminous assemblages. Although gedrite is no longer in contact with sillimanite, it once was, and so it can be plotted in diagrams to allow for the visualization of mineral assemblages and reactions before and during the formation of the enclaves as well as all the reactions involving sillimanite. However, when using real compositions of minerals instead of idealized compositions, this projection does not work well to represent the corona assemblages present in gedrite – cordierite – garnet rocks from Evergreen, as three of the minerals, corundum, hercynite, and staurolite, plot in a negative sense. Alternative chemographic representations consist of projecting from corundum or quartz. A projection from corundum allows for the representation of some of the corona assemblages and the visualization of the mineral reactions involving corundum. However, the matrix phases garnet and gedrite do not coexist (only gedrite may once have coexisted) with corundum and, therefore, a projection of these minerals would be invalid. The second alternative, which involves a projection from quartz onto the plane defined by $[Al_2O_3 – (Na_2O + CaO)] – MgO – (FeO + ZnO + MnO)$, permits the representation of the matrix assemblages and works well to represent most mineral reactions (Fig. 7c). The result of adding ZnO + MnO, and subtracting Na_2O + CaO, is to minimize the effect of these extra components in the projection of hercynite, staurolite, gedrite, and garnet.

Interpretation Of Textures And Metamorphic Reactions

On the basis of detailed textural studies of corona and matrix associations and chemical compositions of coexisting minerals obtained from electron-microprobe analyses, a set of linear equations in the system $FeO – MgO – Al_2O_3 – SiO_2 \pm ZnO \pm TiO_2 \pm MnO \pm S_2$ (FMAS ± ZTMnSulfur) can be solved by matrix

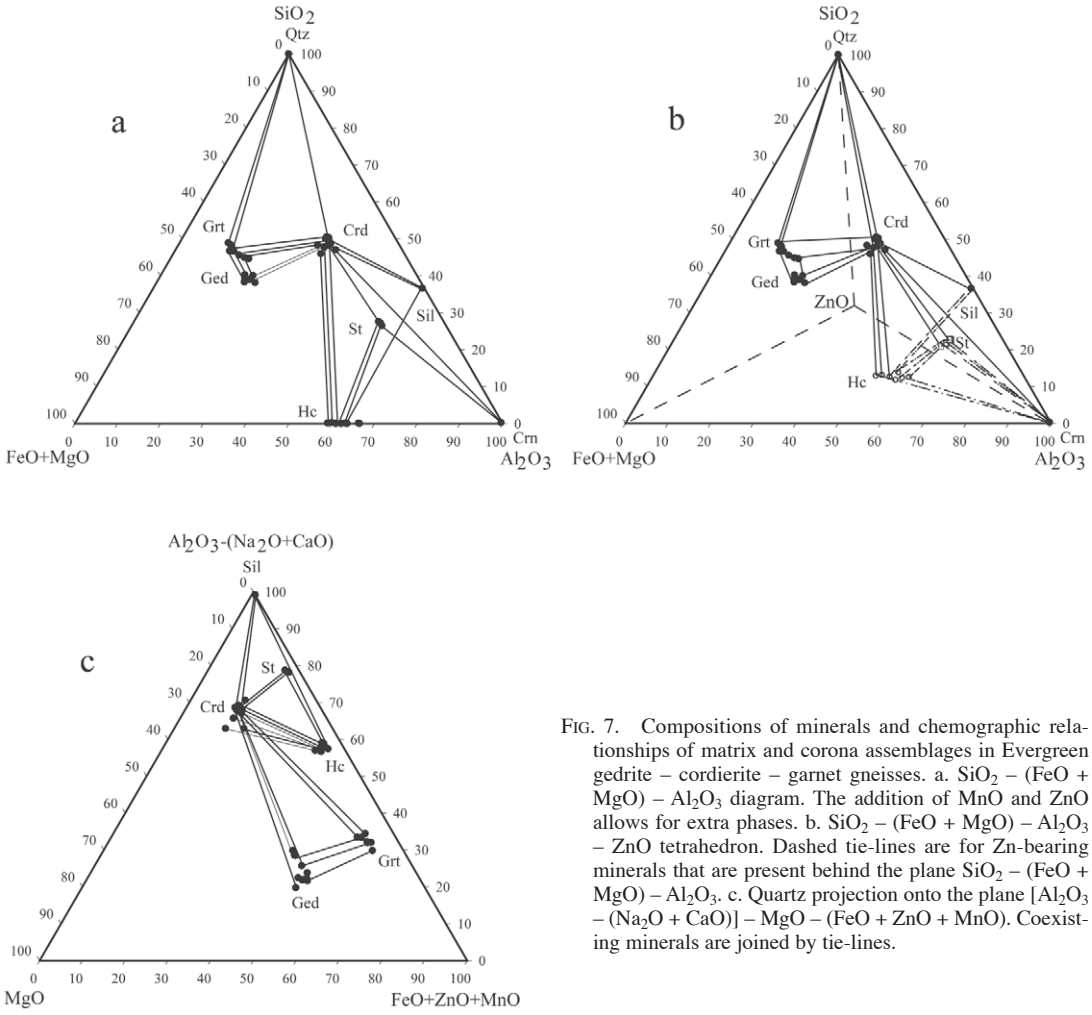

FIG. 7. Compositions of minerals and chemographic relationships of matrix and corona assemblages in Evergreen gedrite – cordierite – garnet gneisses. a. SiO_2 – (FeO + MgO) – Al_2O_3 diagram. The addition of MnO and ZnO allows for extra phases. b. SiO_2 – (FeO + MgO) – Al_2O_3 – ZnO tetrahedron. Dashed tie-lines are for Zn-bearing minerals that are present behind the plane SiO_2 – (FeO + MgO) – Al_2O_3. c. Quartz projection onto the plane [Al_2O_3 – (Na_2O + CaO)] – MgO – (FeO + ZnO + MnO). Coexisting minerals are joined by tie-lines.

analysis to obtain a set of balanced metamorphic reactions among the mineral phases. This matrix analysis performed with compositions of minerals in the systems FMA, FMAZ, FMAZMnSulfur, FMAZSulfur, and FTA (depending on the phases involved), coupled with the textural investigations, allow for the identification of a set of reactions that occurred during the evolution of the gedrite – cordierite – garnet rocks at Evergreen. The observed and inferred reactions and calculated stoichiometric coefficients are listed in Table 4.

Gedrite + sillimanite + garnet + quartz + sphalerite is the precursor assemblage in gedrite – cordierite – garnet rocks, on the basis of the existence of relict (corroded) sillimanite crystals in the center of the coronas that are nowhere in contact with the matrix assemblage gedrite – garnet, and of quartz inclusions in cordierite, gedrite, and garnet (Fig. 8a). Cordierite formed as a replacement along the cleavage planes of gedrite and was, therefore, not part of the precursor assemblage. Sphalerite was the likely precursor to zincian hercynite owing to its presence as tiny inclusions in hercynite and sillimanite in gedrite – cordierite – garnet rocks and surrounding rocks, and the absence of zinc in any of the precursor silicates.

On the basis of the above considerations, we started by calculating a simplified reaction in the system FMA ignoring zinc-bearing phases:

$$0.73 \text{ gedrite} + 0.46 \text{ sillimanite} = 0.35 \text{ garnet} + 1.00 \text{ cordierite (system FMA).} \quad (1)$$

Note that mineral formulas were based on 23 atoms of oxygen for gedrite, 20 for sillimanite, 24 for garnet, and 18 for cordierite. By using these values, which are

20 or nearly 20 atoms of oxygen, coefficients in the reaction approximate modal proportions (and therefore volumes) of reactant and product phases (Thompson 1982b). Reaction (1), which is shown by dashed lines in a quartz projection in $[Al_2O_3 - (Na_2O + CaO)] - MgO - [FeO + ZnO + MnO]$ space in Figure 8a, was first proposed by Grant (1968) and Hudson & Harte (1985), and mentioned by Gable & Sims (1969) in their description of gedrite-bearing gneisses from the Front Range. Chemographic relationships indicate that reaction (1) can account for the presence of the common assemblage gedrite – cordierite – garnet – quartz in the matrix, and for the formation of garnet and cordierite that grew at the expense of gedrite in the matrix. Cordierite also nucleated close to sillimanite, next to older grains of garnet, and forming cordierite coronas around gedrite.

In order to take into account the widespread presence of hercynite within the coronas (Figs. 4d, e), we modified reaction (1) to include Zn. As noted above, we assumed that, prior to development of hercynite, Zn was contained mainly within sphalerite. In other words, this modification involves the addition of one component (Zn), but two phases (sphalerite and hercynite). Consequently, the system cannot be balanced without the consideration of an additional component (S_2 cannot serve this purpose because its activity is assumed to be fixed by the amount of sphalerite). We chose Mn for this purpose, which led to the following reaction (Fig. 8a):

0.74 gedrite + 0.77 sillimanite + 0.26 sphalerite
= 0.09 garnet + 1.00 cordierite + 0.36 hercynite
+ 0.26 S_2 (FMAMnZSulfur). (2)

Following the reasoning outlined above for balancing reactions, the formula for hercynite was calculated assuming 20 atoms of oxygen. Reaction (2) is consistent with the clear textural evidence for the consumption of gedrite and sillimanite and the production of substantial cordierite during formation of the coronas, as well as with the widespread association of hercynite with cordierite in the coronas. However, reaction (2) predicts a ratio of hercynite to cordierite far greater than that actually observed. We attribute this to the role of Mn in constraining the reaction coefficients. Because of the low Mn content of gedrite and sillimanite, reaction (2) can generate only a limited amount of garnet. This, in turn, forces an unrealistically large coefficient for hercynite, because the Mg/Fe value of cordierite is much higher than that of gedrite. We consider that the above problem arises because the Mn content utilized for garnet may represent that of the prograde composition of this phase, rather than that produced during the corona-forming reaction. Hence, we also calculated a variant of reaction (2) in which we forced the proportions of cordierite and hercynite in the coronas to be 90% and 10%, respectively, on the basis of petrographic observations. Fixing this ratio reduces the number of unknowns and allows the mass-balance equations to be solved without considering Mn:

0.73 gedrite + 0.56 sillimanite + 0.07 sphalerite
= 0.27 garnet + 1.00 cordierite
+ 0.11 hercynite + 0.04 S_2 (FMAZSulfur). (3)

Note that this reaction produces a greater amount of garnet per unit of cordierite than is the case for reaction (2), but less than reaction (1).

The nucleation of cordierite adjacent to sillimanite by reactions (2) and (3) is probably due to the low rate of diffusion of Al (*e.g.,* Mongkoltip & Ashworth 1983, Schumacher & Robinson 1987). However, since the cordierite shell grew in close proximity to gedrite, the low diffusivity of Mg was probably also important for its nucleation. Like cordierite, the nucleation of hercynite was dependent upon the low rate of diffusion of Al, and it formed next to sillimanite. The result of the diffusion-controlled reaction is a shell of cordierite of almost constant width around sillimanite that is locally intergrown with hercynite in worm-like symplectites. Reactions (2) and (3) also explain the presence of coexisting hercynite and cordierite in sillimanite-bearing and sillimanite-absent samples (Figs. 4e, 8a). In the latter samples, sillimanite was either consumed during the progress of these reactions, or it is not observed in the small area of the thin section. The appearance of the assemblage cordierite – hercynite – sillimanite reflects a more aluminum-rich domain than where garnet, gedrite, and cordierite are dominant. This mineralogical variation, however, is a local effect produced by the nucleation of minerals next to available sillimanite, which was not abundant in the original assemblage, as indicated by the small volume occupied by the enclaves and the absence of this mineral in some of the rocks.

TABLE 4. REACTIONS AND STOICHIOMETRIC COEFFICIENTS FOR THE EQUILIBRIA DISCUSSED IN THE TEXT

Sample	Reaction	System	Equation
65A	0.73 ged + 0.46 sil = 0.35 grt + 1.00 crd	AFM	(1)
65A	0.74 ged + 0.77 sil + 0.26 sph = 0.09 grt + 1.00 crd + 0.36 hc + 0.26 S_2	FMAMnZSulfur	(2)
65A	0.73 ged + 0.56 sil + 0.07 sph = 0.27 grt + 1.00 crd + 0.11 hc + 0.04 S_2	FMAZSulfur	(3)
AHCO-7	0.75 ged + 0.46 sil + 0.04 sph + 0.02 qtz = 0.31 grt + 1.00 crd + 0.06 hc + 0.06 crn + 0.02 S_2	FMASZSulfur	(4)
64	0.35 sil + 0.07 hc = 0.16 st + 1.00 crn	FMA	(5)
65A	3.67 grt + 11.96 sil + 1.00 crd = 11.73 st	FMA	(6)
65A	2.97 grt + 11.58 sil + 1.00 crd + 1.11 hc = 12.26 st	FMAZ	(7)
65B	0.71 hc + 4.77 ilm + 3.12 crn = 1.00 hog	FTA	(8)

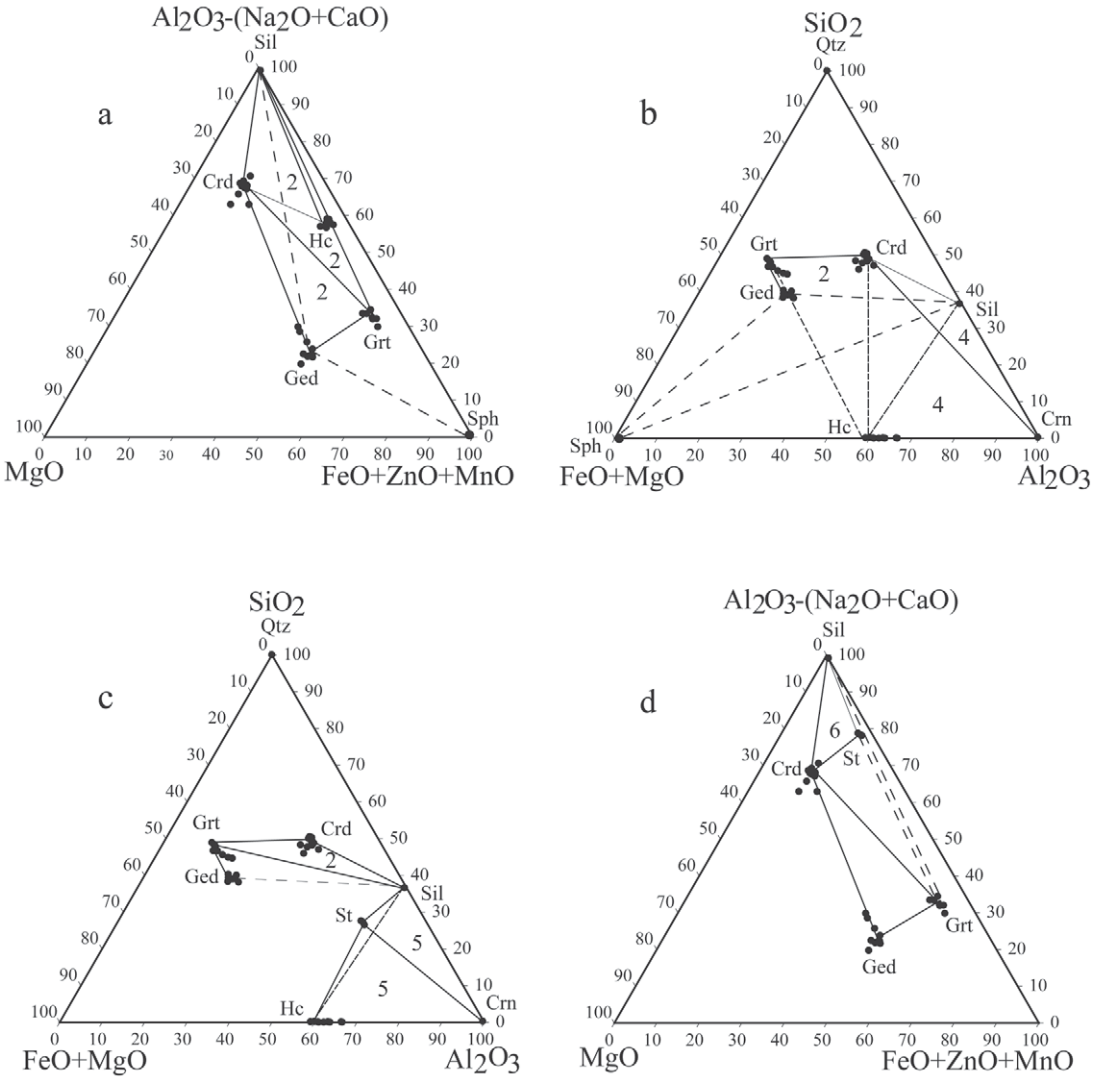

FIG. 8. Metamorphic reactions for Evergreen gedrite – cordierite – garnet gneisses shown in projections in the systems [Al_2O_3 – (Na_2O + CaO)] – MgO – (FeO + ZnO + MnO) from quartz (a, d) and SiO_2 – (FeO + MgO) – Al_2O_3 (b, c). Diagrams show the formation of cordierite – garnet, hercynite, corundum, and staurolite by the following reactions starting from gedrite + sillimanite (dashed tie-line): a) ged + sil + sph = grt + crd + hc + S_2, b) ged + sil + sph = grt + crd + hc + crn + S_2, c) sil + hc = crn + st, d) crd + grt + sil = st. Numbers refer to reactions in the text and Table 4. The addition of MnO and ZnO in b) and c) will slightly shift the positions of garnet and hercynite, respectively. Long dashed tie-lines indicate reactant and precursor phases. Short dashed lines are for Zn-bearing minerals. See text and Table 4 for a discussion of reactions and further details.

The presence of corundum in the center of enclaves that contain hercynite and cordierite also requires a reaction in which gedrite, sillimanite, quartz, and sphalerite are consumed. Taking into account the proportion of corundum, hercynite and cordierite in the enclave, the corundum-forming reaction is:

0.75 gedrite + 0.46 sillimanite
+ 0.04 sphalerite + 0.02 quartz = 0.31 garnet
+ 1.00 cordierite + 0.06 hercynite
+ 0.06 corundum + 0.02 S_2 (FMASZSulfur). (4)

Reaction (4) is schematically shown in Figure 8b and is texturally supported by the presence of sillimanite

inclusions in corundum, and the existence of the assemblage corundum – sillimanite – cordierite (Figs. 4f, g). In places, corundum and cordierite occur as pseudomorphs after sillimanite next to relict sillimanite, whereas hercynite is located in the outer zone of the enclave (Fig. 4f). The ragged appearance of corundum in places indicates that this mineral was subsequently unstable, probably because it reacted further (Figs. 4e, f). The presence of ZnO, which permits the stabilization of a five-phase assemblage, and the partial completion of reaction (4), make it possible to preserve the metastable association sillimanite – hercynite, as long as they are isolated from gedrite by the cordierite corona. However, the enclave texture also allows for the formation of corundum *via* the breakdown of sillimanite and hercynite (Fig. 8c):

0.35 sillimanite + 0.07 hercynite
= 0.16 staurolite + 1.00 corundum (FMA). (5)

As a result of reactions (1) to (4), the assemblage garnet – sillimanite – cordierite was probably stable until the completion of the growth of the cordierite shell between gedrite and sillimanite. The presence of staurolite in the coronas could have resulted from reaction (5) as well as the following reaction (Fig. 8d):

3.67 garnet + 11.96 sillimanite
+ 1.00 cordierite = 11.73 staurolite (FMA). (6)

However, the small amount of zinc present in staurolite was likely derived from hercynite *via* the following reaction:

2.97 garnet + 11.58 sillimanite + 1.11 hercynite
+ 1.00 cordierite = 12.26 staurolite (FMAZ). (7)

It is worth noting that a staurolite-forming reaction but without hercynite as a reactant was proposed by Robinson & Jaffe (1969) and Hudson & Harte (1985) to explain the origin of aluminous enclaves in samples from New Hampshire and northeast Scotland (Buchan Dalradian), respectively. However, these authors did not consider the ZnO component of the system. Reaction (7) accounts for the presence of Zn in hercynite and staurolite, hercynite inclusions in staurolite and cordierite, staurolite pseudomorphs after sillimanite next to relict sillimanite, and the assemblage staurolite – cordierite (Figs. 4f, g). Staurolite nucleated close to hercynite, cordierite, corundum, and sillimanite in the corona. The fact that staurolite and corundum appear in close spatial association indicates that corundum may have been a reactant in the staurolite-forming reaction, but intermediate steps between the earlier formation of hercynite and corundum, as well as the origin of staurolite, cannot be deduced. Therefore, the amount of corundum in the possible staurolite-forming reaction remains unknown. The completion of this reaction ended the association hercynite – sillimanite and explains the absence of sillimanite in some samples, where it was consumed. Where reaction (7) did not reach completion, sillimanite was preserved as relics spatially associated with hercynite (Figs. 4d, e, f). Although topological relationships suggest that the assemblage staurolite – cordierite – sillimanite was stable, staurolite and sillimanite were never observed in mutual contact.

The presence of staurolite in some rocks and not in others can be explained by local variations in chemical composition; an enrichment in Fe was favorable for its growth. As a result of reactions (5), (6), and (7), the local composition becomes more aluminum-rich than that represented by the matrix phases. Upon completion of reaction (4) and the formation of staurolite and the other minerals in the corona, cordierite will isolate all the aluminous minerals from gedrite and end the association gedrite – sillimanite – garnet.

A rim of högbomite developed along the contact between ilmenite and hercynite (Fig. 4h) and adjacent to corundum, and probably formed by the following reaction that took place during retrograde metamorphism:

0.71 hercynite + 4.77 ilmenite
+ 3.12 corundum = 1.00 högbomite (FTA). (8)

The reaction was also balanced in the system AFZ. The formation of högbomite by this reaction explains the corroded appearance of corundum and the intimate spatial association among all four minerals. According to Petersen *et al*. (1989), reaction (8) is a pressure-independent reaction.

Thermobarometry

Temperatures and pressures were calculated using mineral compositions, mineral stabilities, and geothermometers based on the assemblages garnet – cordierite, spinel – cordierite, and spinel – cordierite – sillimanite – quartz. Reactions and mineral assemblages utilized are based on textural interpretations. The lower stability-limit of the assemblage gedrite + sillimanite + garnet + quartz, as indicated by the reaction line:

staurolite = gedrite + sillimanite + garnet (9)

suggests that peak pressures and temperatures of metamorphism were >5 kbar and 680°C, respectively (Fig. 9). Utilizing T–*X* solvi for orthoamphiboles (Spear 1980, Fig. 14), gedrite – ferrogedrite compositions (^{IV}Al = 1.02 to 1.89 *apfu*; ^{VI}Al = 0.32 to 1.29 *apfu*; *A*-site occupancy = 0.24 to 0.54 *apfu*, Fig. 5b) suggest a minimum temperature of orthoamphibole formation of 520–590°C. A temperature of ~583°C is obtained by the intersection of the orthoamphibole solvus, which indicates the lower-temperature limit for the presence of gedrite (Spear 1993; Fig. 9, this work):

gedrite + anthophyllite = orthoamphibole, (10)

with the reaction

andalusite = sillimanite. (11)

The upper stability-field of staurolite, assuming excess quartz, as dictated by reaction (6), coincides with the lower limit of the garnet – cordierite assemblage of 680ºC at 5 kbar (Fig. 9). However, the upper temperature of 680ºC may be a minimum, as staurolite contains up to 0.9 wt.% ZnO, which would cause reaction (5) to shift to slightly higher temperatures. The intersection of reaction (6) with reaction (11) indicates a minimum retrograde pressure for the stability of staurolite in the presence of sillimanite of approximately 2 kbar (Fig. 9).

The garnet – cordierite geothermometer is based on experimental or empirical calibrations of the following exchange-equilibria (Thompson 1982a):

$$MgFe_{-1}\ [\text{cordierite}] = MgFe_{-1}\ [\text{garnet}]. \quad (12)$$

It was applied to samples in the present study, and temperatures were calculated at 2 and 5 kbar, which is the range of pressures estimated from reaction (1) and the intersection of reactions (6) and (11). The garnet – cordierite geothermometer applied to eleven garnet – cordierite pairs from five samples yielded temperatures of 629–673°C at 5 kbar and 616–659°C at 2 kbar (Table 5), using the calibration of Bhattacharya *et al.* (1988).

The association of spinel with sillimanite, cordierite, and quartz in the corona assemblage allows for the application of the spinel – sillimanite – cordierite – quartz geothermometer of Nichols *et al.* (1992). Temperatures obtained from seven hercynite – cordierite pairs in three samples are 482 to 608°C at 5 kbar and 468 to 593°C at 2 kbar. Application of the spinel – cordierite pressure-independent geothermometer of Vielzeuf (1983) to twelve spinel – cordierite pairs in four samples yielded temperatures of 567 to 780°C.

Discussion and Conclusions

The stability fields of sillimanite + garnet + gedrite + cordierite [reactions (9) and (1)] indicate peak conditions of metamorphism of above 5 kbar and 680°C. On the basis of the stability of staurolite [reaction (6)], coupled with the minimum temperature of 580ºC derived from the presence of gedrite, the P–T conditions recorded in cordierite – gedrite rocks at the time of corona formation in the Evergreen area are approximately 590–680ºC and 2.0–5.0 kbar. These conditions are similar to P–T estimates (620–710ºC at 3–5 kbar) for rocks in the Central City area, 25 km northeast of Evergreen (Gable & Sims 1969). Considering that staurolite formed after peak conditions later than hercynite and corundum, and because the presence of minor amounts of Zn in staurolite expands its field of stability,

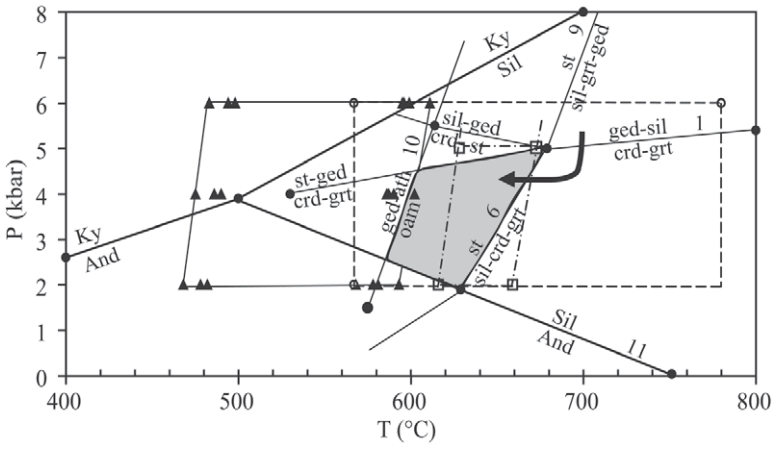

FIG. 9. P–T diagram in the system FMAS showing reactions pertinent to cordierite – orthoamphibole rocks (Spear 1993), calculated geothermobarometry values, recorded peak-to-retrograde P–T conditions (shaded area), and a possible P–T path for Evergreen gedrite – cordierite – garnet gneisses. Reaction numbers are the same as those in the text. The symbols indicate:

____ ▲ Spl–crd–sil–qtz geothermobarometry (Nichols *et al.* 1992)
- - - - ○ Spl–crd geothermometry (Vielzeuf 1983)
- • - • □ Grt–crd geothermometry (Bhattacharya *et al.* 1988)

the upper-temperature limit might be even higher than this estimate. Temperatures obtained from the following geothermometers: garnet – cordierite (629–673°C at 5 kbar and 616–659°C at 2 kbar), spinel – cordierite (567–780°C), and spinel – sillimanite – cordierite – quartz (482–608°C at 5 kbar and 468–593°C at 2 kbar), overlap with the range of estimates given above. However, the lowest temperatures obtained from spinel – sillimanite – cordierite – quartz geothermometry must be in error, as they are <504 ± 20ºC (*i.e.,* aluminosilicate triple point of Holdaway & Mukhopadhyay 1993), and must fall within the stability fields of kyanite or andalusite. This low-temperature estimate may in part be due to the low content of quartz and its exclusive presence as inclusions within cordierite in the corona, and possible errors associated with the calibration of the geothermometer proposed by Nichols *et al*. (1982). The problem is exacerbated if the aluminosilicate triple point of 550ºC and 4.5 kbar of Pattison (2001) is preferred. The temperature range of the garnet – cordierite geothermometer fits within the range of temperatures derived from silicate stabilities, indicating that equilibration of these minerals probably took place after the formation of staurolite. The upper temperature obtained from the spinel – cordierite geothermometer is considerably higher than this range and the upper stability-limit of staurolite, which is consistent with the idea that hercynite formed prior to staurolite. The reason for the broad range of temperatures obtained with the spinel – cordierite geothermometer remains uncertain, but Vielzeuf (1983) claimed that the geothermometer was best used for granulite-facies rocks, rather than amphibolite-facies rocks, and pointed out that the distribution coefficients (and hence the error of uncertainty) for the spinel – cordierite calibration are more dispersed at amphibolite-facies conditions. However, the broad range of temperatures may also be due to the presence of Zn in hercynite, which affects the calibration, as well as the low rate of diffusion of aluminum in hercynite, which could have prevented re-equilibration as temperatures fell.

Robinson & Jaffe (1969), Schumacher & Robinson (1987), Clarke *et al*. (1989), Yardley (1989), Passchier & Trouw (1996), Cadéron *et al*. (2005), and Yang & Indares (2005) provided considerable evidence to support the concept that aluminous coronas and symplectites in rocks metamorphosed to the upper amphibolite to granulite facies formed after peak metamorphism during a period of decompression associated with substantial exhumation. In addition, Baker *et al*. (1987) explained the origin of corona textures in kyanite – garnet – gedrite gneisses by a set of reactions that took place during uplift and little cooling. However, these are alternative interpretations. Clarke & Powell (1991) and Brown (2002) suggested that coronas may have formed along a "normal" path of retrograde cooling; according to Pitra & De Waal (2001), they may even have formed during prograde metamorphism.

Textural and compositional studies of symplectites and coronas in gedrite – cordierite – garnet rocks at Evergreen suggest that they formed *via* a complex set of discontinuous, continuous, and diffusion-controlled reactions in the system FMAMnZSulfur from the assemblage gedrite – sillimanite – garnet – quartz – sphalerite. The reactions proposed herein help explain: 1) the presence of relict sillimanite crystals in the center of the coronas, 2) the presence of cordierite cross-cutting gedrite and the formation of minor garnet in the matrix, 3) the formation of hercynite – cordierite symplectites between sillimanite and gedrite, 4) the cordierite shell around the Al-rich minerals, which separates them from gedrite and garnet, 5) hercynite inclusions within corundum and staurolite, and sillimanite inclusions in corundum, 6) hercynite – cordierite, and corundum

TABLE 5. TEMPERATURES OBTAINED FROM THE GARNET – CORDIERITE GEOTHERMOMETER

Sample	K_D[1]	B88[2,3] (°C)	B88[2,4] (°C)
AHCO6	0.09	654	640
	0.10	673	659
AHCO5	0.08	636	623
	0.08	629	616
AHCO7	0.08	651	638
	0.08	658	645
99CO65B	0.09	670	657
	0.08	650	637
	0.08	655	642
99CO65A	0.09	667	654
	0.08	642	630

[1] $K_D = (X_{Fe} / X_{Mg})^{crd} / (X_{Fe} / X_{Mg})^{grt}$.
[2] Calculations performed using the calibration (B88) of Bhattacharya *et al*. (1988).
[3] Temperatures determined at 5 kbar. [4] Temperatures determined at 2 kbar.

TABLE 6. TEMPERATURES AND CORRESPONDING PRESSURES OBTAINED FROM SPINEL – CORDIERITE – SILLIMANITE – QUARTZ GEOTHERMOBAROMETER*

Sample	T (°C)	P (kbar)	Sample	T (°C)	P (kbar)
AHCO5	468	2	99CO65A	608	5
	475	4		611	6
	482	5			
	483	6	99CO64	482	2
				490	4
99CO65A	478	2		494	5
	486	4		498	6
	490	5		581	2
	494	6		590	4
	568	2		595	5
	586	4		599	6
	592	5		578	2
	595	6		587	4
	593	2		594	5
	602	4		596	6

* Using the calibration of Nichols *et al*. (1992).

– staurolite – cordierite pseudomorphs after sillimanite, and 7) grains of högbomite between hercynite and ilmenite where spatially associated with corundum.

On the basis of the inferred set of texturally supported reactions, we suggest that coronas and symplectites formed after the peak conditions of metamorphism were reached. The earliest metamorphic assemblage gedrite – garnet – sillimanite (in the system FMAMn) requires initial P–T conditions to have been located above reaction (1) at P > 5 kbar and on the higher-temperature side of reaction (9) above 680ºC (Fig. 9). Reaction (1) has a relatively flat slope indicating that an increase in volume takes place during decreasing pressure. Therefore, starting in the gedrite – sillimanite – garnet field, the formation of cordierite + garnet by reaction (1) is associated with a period of decompression (Fig. 9). Zincian hercynite formed during the same overall reaction as a result of the presence of Zn in the system. The formation of cordierite – hercynite symplectites and the cordierite corona are consistent with this retrograde period of decompression that took place starting at 5 kbar. The subsequent formation of staurolite from the assemblage cordierite + garnet + sillimanite [reaction (6)] requires the P–T path to cross toward lower temperatures (Fig. 9). The result of this sequence of reactions is a clockwise path that ends in the field where staurolite is stable and represents the corona assemblage.

We consider that most of the minerals in the coronas and the hercynite – cordierite symplectites present in Evergreen gedrite – cordierite – garnet gneisses formed during this path of decompression and subsequent cooling. The nearly isothermal reaction (8) (Petersen *et al*. 1989) associated with the formation of högbomite probably occurred during cooling after the formation of the coronas.

The intrusion of the Boulder Creek Granite pluton at 1,710 Ma (Hedge 1969, Premo & Fanning 2000) 5 km south of Evergreen overlaps the age of metamorphism of 1,775 to 1,700 Ma (Hedge *et al*. 1967), but this intrusive event appears to have caused only local contact effects. However, if we assume the location of the boundary zone between the Yavapai and Mazatzal provinces of Shaw & Karlstrom (1998) and accept their proposal that the Yavapai province overthrusted the Mazatzal province, the Evergreen area, located in the Yavapai province, was likely affected by rapid uplift. This assumption can be related to interpretations of 1.70–1.65 Ga post-collisional decompressional history and metamorphism inferred for the Mazatzal province (Williams & Karlstrom 1996, Selverstone *et al*. 1999). Such a scenario would explain the formation of the corona and symplectitic textures, which are, in general, associated with regions of rapid decompression. We note here that this reconstruction is in disagreement with a counter-clockwise P–T path proposed by Selverstone *et al*. (1999) for the evolution of Proterozoic crustal rocks beneath the Colorado Plateau on the basis of textural evidence from xenoliths in Tertiary diatremes. Alternatively, the intrusion of 1,440 Ma granite rocks (Silver Plume Granite) about 5 km southeast of the study area may also have played a role in the generation of the corona textures and mineral growth during exhumation, consistent with geochronological data and interpretations of a metamorphic event at about 1.4 Ga in the Wet Mountains (Siddoway *et al*. 2000).

TABLE 7. TEMPERATURES OBTAINED FROM THE SPINEL–CORDIERITE GEOTHERMOMETER

Sample	Spinel		Cordierite		X_{Mg}^{spl}	X_{Fe}^{spl}	X_{Mg}^{crd}	X_{Fe}^{crd}	$K_D^{spl\text{-}crd}$ [1]	T °C [2]
	Mg	Fe	Mg	Fe						
AHCO5	0.16	0.64	1.48	0.50	0.20	0.80	0.75	0.25	0.08	567
	0.17	0.60	1.41	0.54	0.21	0.79	0.73	0.27	0.10	659
99CO65A	0.30	0.73	1.71	0.54	0.29	0.71	0.76	0.24	0.13	779
	0.29	0.79	1.80	0.57	0.27	0.73	0.76	0.24	0.12	719
	0.17	0.72	1.45	0.53	0.20	0.80	0.73	0.27	0.09	588
	0.19	0.72	1.40	0.55	0.20	0.80	0.72	0.28	0.10	642
99CO64	0.19	0.74	1.44	0.51	0.20	0.80	0.74	0.26	0.09	589
	0.22	0.65	1.44	0.52	0.26	0.74	0.74	0.26	0.12	756
	0.22	0.67	1.42	0.52	0.25	0.75	0.73	0.27	0.12	747
	0.18	0.61	1.41	0.52	0.23	0.77	0.73	0.27	0.11	697
AHCO6	0.19	0.69	1.47	0.51	0.21	0.79	0.74	0.26	0.09	613
	0.19	0.68	1.51	0.53	0.22	0.78	0.74	0.26	0.10	640

[1] $K_D = (X_{Mg}^{spl} \bullet X_{Fe}^{crd}) / (X_{Fe}^{spl} \bullet X_{Mg}^{crd})$.
[2] $T(K) = -1,763 / (\ln K_D + 0.378)$; calibration of Vielzeuf (1983).
Amounts of Mg and Fe are expressed in atoms per formula unit.

ACKNOWLEDGEMENTS

Discussions with Tom Foster and Jane Dawson helped clarify our understanding of the origin of corona and symplectite textures, whereas communications with Frank Spear clarified aspects of our reaction-modeling procedures. The manuscript was improved by the comments of Robert Martin and Walt Trzcienski. Field and analytical costs were supported by Lynch Mining and by a Hugh E. McKinstry Student Research Grant from the Society of Economic Geologists to A.H. An Organization of American States Fellowship (PRA, Uruguay) to A.H. is gratefully appreciated.

REFERENCES

ARAUJO, S.M., FAWCETT, J.J. & SCOTT, S.D. (1995): Metamorphism of hydrothermally altered rocks in a volcanogenic massive sulfide deposit: the Palmeiropolis, Brazil, example. *Rev. Bras. Geociências* **25**, 173-184.

BAKER, J., POWELL, R., SANDIFORD, M. & MUHLING, J. (1987): Corona textures between kyanite, garnet, and gedrite in gneisses from Errabiddy, Western Australia. *J. Metamorph. Geol.* **5**, 357-370.

BENNETT, V.C. & DEPAOLO, D.J. (1987): Proterozoic crustal history of the western United States as determined by neodymium isotopic mapping. *Geol. Soc. Am., Bull.* **99**, 674-685.

BHATTACHARYA, A., MAZUMDAR, A.C. & SEN, S.K. (1988): Fe–Mg mixing in cordierite: constraints from natural data and implications for cordierite–garnet geothermometry in granulites. *Am. Mineral.* **73**, 338-344.

BROWN, M. (2002): Retrograde processes in migmatites and granulites revisited. *J. Metamorph. Geol.* **20**, 25-40.

CADÉRON, S., TRZCIENSKI, W.E., JR., BÉDARD, J.H. & GOULET, N. (2005): An occurrence of sapphirine in the Archean Superior Province, northern Quebec. *Can. Mineral.* **43**, 463-478.

CLARKE, G.L. & POWELL, R. (1991): Decompressional coronas and symplectites in granulites of the Musgrave Complex, central Australia. *J. Metamorph. Geol.* **9**, 441-450.

CLARKE, G.L., POWELL, R. & GIRAUD, M. (1989): Low-pressure granulite facies metapelitic assemblages and corona textures from MacRobertson Land, east Antarctica: the importance of Fe_2O_3 and TiO_2 in accounting for spinel-bearing assemblages. *J. Metamorph. Geol.* **7**, 323-335.

CONDIE, K.C. (1982): Plate-tectonic model for Proterozoic continental accretion in the southwestern United States. *Geology* **10**, 37-42.

DAMMAN, A.H. (1989): Hydrothermal orthoamphibole-bearing assemblages from the Gåsborn area, West Bergslagen, central Sweden. *Am. Mineral.* **74**, 573-585.

DEER, W.A., HOWIE, R.A. & ZUSSMAN, J. (1966): *Rock-Forming Minerals*. **1**. *Ortho- and Ring Silicates*. Longmans, London, U.K.

DROOP, G.T.R. (1987): A general equation for estimating Fe^{3+} concentrations in ferromagnesian silicates and oxides from microprobe analyses, using stoichiometric criteria. *Mineral. Mag.* **51**, 431-435.

EARLEY, D., III & STOUT, J. (1991): Cordierite–cummingtonite facies rocks from the Gold Brick District, Colorado. *J. Petrol.* **32**, 169-1201.

GABLE, D.J. & SIMS, P.K. (1969): Geology and regional metamorphism of some high-grade cordierite gneisses, Front Range, Colorado. *Geol. Soc. Am., Spec. Pap.* **128**, 1-87.

GRANT, J.A. (1968): Partial melting of common rocks as a possible source of cordierite–anthophyllite-bearing assemblages. *Am. J. Sci.* **266**, 908-931.

GREENWOOD, H.J. (1975): Thermodynamically valid projections of extensive phase relationships. *Am. Mineral.* **60**, 1-8.

HEDGE, C.E. (1969): *A Petrogenetic and Geochronologic Study of Migmatite and Pegmatites in the Central Front Range*. Ph.D. thesis, Colorado School of Mines, Golden, Colorado.

HEDGE, C.E., HOUSTON, R.S., TWETO, O.L., PETERMAN, Z.E., HARRISON, J.E. & REID, R.R. (1986): The Precambrian of the Rocky Mountain region. Correlation of Precambrian rocks of the United States and Mexico. *U.S. Geol. Surv., Prof. Pap.* **1241–D**, 551-558.

HEDGE, C.E., PETERMAN, Z.E. & BRADDOCK, W.A. (1967): Age of the major Precambrian regional metamorphism in the northern Front Range, Colorado. *Geol. Soc. Am., Bull.* **78**, 551-558.

HEIMANN, A. (2002): *Zinc-Rich Spinels Associated with Proterozoic Base Metal Sulfide Occurrences, Colorado, and Their Use as Guides to Metamorphosed Massive Sulfide Deposits*. M.S. thesis, Iowa State University, Ames, Iowa.

HEIMANN, A., SPRY, P.G. & TEALE, G.S. (2005): Zincian spinel associated with Proterozoic base-metal sulfide occurrences, Colorado: a re-evaluation of gahnite composition as a guide in exploration. *Can. Mineral.* **43**, 601-622.

HOLDAWAY, M.J. & MUKHOPADHYAY, B. (1993): A reevaluation of the stability relations of andalusite: thermochemical data and phase diagram for the aluminum silicates. *Am. Mineral.* **78**, 298-315.

HUDSON, N.F.C. & HARTE, B. (1985): K_2O-poor, aluminous assemblages from the Buchan Dalradian, and the variety of orthoamphibole assemblages in aluminous bulk compositions in the amphibolite facies. *Am. J. Sci.* **285**, 224-266.

JAMES, R.S., GRIEVE, R.A.F. & PAUK, L. (1978): The petrology of cordierite-anthophyllite gneisses and associated mafic and pelitic gneisses at Manitouwadge, Ontario. *Am. J. Sci.* **278**, 41-63.

KARLSTROM, K.E. (1998): Introduction to special issues: lithospheric structure and evolution of the Rocky Mountains (Part I and II). *Rocky Mountain Geol.* **33**, 157-159.

KARLSTROM, K.E. & HUMPHREYS, E.D. (1998): Persistent influence of Proterozoic accretionary boundaries in the tectonic evolution of southwestern North America: interaction of cratonic grain and mantle modification events. *Rocky Mountain Geol.* **33**, 161-179.

LEAKE, B.E. & 21 others (1997): Nomenclature of amphiboles: report of the subcommittee on amphiboles of the International Mineralogical Association, Commission on New Minerals and Mineral Names. *Am. Mineral.* **82**, 1019-1037.

LOVERING, T.S. & GODDARD, E.N. (1950): Geology and ore deposits of the Front Range, Colorado. *U.S. Geol. Surv., Prof. Pap.* **223**, 1-319.

MARSH, S.P. & SHERIDAN, D.M. (1976): Rutile in Precambrian sillimanite–quartz gneiss and related rocks, east-central Front Range, Colorado. Geology and resources of titanium in the United States. *U.S. Geol. Surv., Prof. Pap.* **959-G**.

MONGKOLTIP, P. & ASHWORTH, J.R. (1983): Quantitative estimation of an open-system symplectite-forming reaction: restricted diffusion of Al and Si in coronas around olivine. *J. Petrol.* **24**, 635-661.

NICHOLS, G.T., BERRY, R.F. & GREEN, D.H. (1992): Internally consistent gahnitic spinel – cordierite – garnet equilibria in the FMASHZn system: geothermobarometry and applications. *Contrib. Mineral. Petrol.* **111**, 362-377.

OUZEGANE, K., DJEMAI, S. & GUIRAUD, M. (1996): Gedrite-garnet-sillimanite-bearing granulites from Amessmessa area, south In Ouzzal, Hoggar, Algeria. *J. Metamorph. Geol.* **14**, 739-753.

PASSCHIER, C.W. & TROUW, R.A.J. (1996): *Microtectonics*. Springer, Berlin, Germany.

PATTISON, D.R.M. (2001): Instability of Al_2SiO_5 "triple point" assemblages in muscovite + biotite + quartz-bearing metapelites, with implications. *Am. Mineral.* **86**, 1414-1422.

PETERSEN, E.U., ESSENE, E.J., PEACOR, D.R. & MARCOTTY, L.A. (1989): The occurrence of högbomite in high-grade metamorphic rocks. *Contrib. Mineral. Petrol.* **101**, 350-360.

PITRA, P. & DE WAAL, S.A. (2001): High-temperature, low-pressure metamorphism and development of prograde symplectites, Marble Hall Fragment, Bushveld Complex (South Africa). *J. Metamorph. Geol.* **19**, 311-325.

PREMO, W.R. & FANNING, C.M. (2000): SHRIMP U–Pb zircon ages for Big Creek gneiss, Wyoming and Boulder Creek batholith, Colorado: implications for timing of Paleoproterozoic accretion of the northern Colorado province. *Rocky Mountain Geol.* **35**, 31-50.

RIBBE, P.H. (1982): Staurolite. *In* Orthosilicates (P.H. Ribbe, ed.). *Rev. Mineral.* **5**, 171-188.

RICKWOOD, P.C. (1968): On recasting analyses of garnet into end-member molecules. *Contrib. Mineral. Petrol.* **18**, 175-198.

ROBINSON, P. & JAFFE, H.W. (1969): Aluminous enclaves in gedrite–cordierite gneiss from southwestern New Hampshire. *Am. J. Sci.* **267**, 389-421.

ROBINSON, P., SPEAR, F.S., SCHUMACHER, J.C., LAIRD, J., KLEIN, C., EVANS, B.W. & DOOLAN, B.L. (1982): Phase relations in the metamorphic amphiboles: natural occurrence and theory. *In* Amphiboles: Petrology and Experimental Phase Relations (D.R. Veblen & P.H. Ribbe, eds.). *Rev. Mineral.* **9B**, 1-227.

SCHNEIDERMAN, J.S. & TRACY, R.J. (1991): Petrology of orthoamphibole–cordierite gneisses from the Orijärvi area, southwest Finland. *Am. Mineral.* **76**, 942-955.

SCHUMACHER, J.C. & ROBINSON, P. (1987): Mineral chemistry and metasomatic growth of aluminous enclaves in gedrite–cordierite gneiss from southwestern New Hampshire, USA. *J. Petrol.* **28**, 1033-1073.

SELVERSTONE, J., PUN, A. & CONDIE, K.C. (1999): Xenolithic evidence for Proterozoic crustal evolution benteath the Colorado Plateau. *Geol. Soc. Am., Bull.* **111**, 590-606.

SHAW, C.A. & KARLSTROM, K.E. (1999): The Yavapai–Mazatzal crustal boundary in the southern Rocky Mountains. *Rocky Mountain Geol.* **34**, 37-52.

SIDDOWAY, C.S., GIVOT, R.M., BODLE, C.D. & HEIZLER, M.T. (2000): Dynamic versus anorogenic setting for Mesoproterozoic plutonism in the Wet Mountains, Colorado; does the interpretation depend on the level of exposure? *Rocky Mountain Geol.* **35**, 91-111.

SPEAR, F.S. (1980): The gedrite–anthophyllite solvus and the composition limits of orthoamphibole from the Post Pond volcanics, Vermont. *Am. Mineral.* **65**, 1103-1118.

SPEAR, F.S. (1993): *Metamorphic Phase Equilibria and Pressure – Temperature – Time Paths*. Mineralogical Society of America, Washington, D.C.

SPRY, P.G. (1982): An unusual gahnite-forming reaction, Geco base-metal deposit, Manitouwadge, Ontario. *Can. Mineral.* **20**, 549-553.

SPRY, P.G. & SCOTT, S.D. (1986): The stability of zincian spinels in sulfide systems and their potential as exploration guides for metamorphosed massive sulfide deposits. *Econ. Geol.* **81**, 1446-1463.

STODDARD, E.F. (1979): Zinc-rich hercynite in high-grade metamorphic rocks: a product of dehydration of staurolite. *Am. Mineral.* **64**, 736-741.

TAYLOR, R.B., SCOTT, G.R., WOBUS, R.A. & EPIS, R.C. (1975a): Reconnaissance geological map of the Royal Gorge quadrangle, Fremont and Custer counties, Colorado. *U.S. Geol. Surv., Misc. Invest. Map* **I-869**.

TAYLOR, R.B., SCOTT, G.R., WOBUS, R.A. & EPIS, R.C. (1975b): Reconnaissance geological map of the Cotopaxi 15-minute quadrangle, Fremont and Custer counties, Colorado. *U.S. Geol. Surv., Misc. Invest. Map* **I-900**.

THOMPSON, J.B., JR. (1957): The graphical analysis of mineral assemblages in pelitic schists. *Am. Mineral.* **42**, 842-858.

THOMPSON, J.B., JR. (1982a): Composition space: an algebraic and geometric approach. *In* Characterization of Metamorphism Through Mineral Equilibria (J.M. Ferry, ed.). *Rev. Mineral.* **10**, 1-31.

THOMPSON, J.B., JR. (1982b): Composition space: an algebraic and geometric approach. *In* Characterization of Metamorphism Through Mineral Equilibria (J.M. Ferry, ed.). *Rev. Mineral.* **10**, 33-52.

TWETO, O. & SIMS, P.K. (1963): Precambrian ancestry of the Colorado mineral belt. *Geol. Soc. Am., Bull.* **74**, 991-1014.

VIELZEUF, D. (1983): The spinel and quartz associations in high grade xenoliths from Tallante (S.E. Spain) and their potential use in geothermometry and barometry. *Contrib. Mineral. Petrol.* **82**, 301-311.

WILLIAMS, M.L. & KARLSTROM, K.E. (1996): Looping *P-T* paths and high-*T*, low-*P* middle crustal metamorphism: Proterozoic evolution of the southwestern United States. *Geology* **24**, 1119-1122.

WILLNER, A.P., SCHREYER, W. & MOORE, J.M. (1990): Peraluminous metamorphic rocks from the Namaqualand Metamorphic Complex (South Africa): geochemical evidence for an exhalation-related, sedimentary origin in a Mid-Proterozoic rift system. *Chem. Geol.* **81**, 221-240.

YANG, P. & INDARES, A.D. (2005): Mineral zoning, phase relations, and P–T evolution of high-pressure granulites from the Lelukuau Terrane, northeastern Grenville Province, Quebec. *Can. Mineral.* **43**, 443-462.

YARDLEY, B.W.D. (1989): *An Introduction to Metamorphic Petrology*. Longman, New York, N.Y.

Received July 15, 2005, revised manuscript accepted September 1, 2006.